Desalination and Water Treatment
www.deswater.com

doi: 10.5004/dwt.2017.20402

67 (2017) 196–205
March

Modeling of arsenic removal from aqueous solution by means of MWCNT/alumina nanocomposite

Hamid Zarei[a], Simin Nasseri[a,b], Ramin Nabizadeh[a], Farzaneh Shemirani[c], Arash Dalvand[d], Amir Hossein Mahvi[a,e,f,*]

[a]*Department of Environmental Health Engineering, School of Public Health, Tehran University of Medical Sciences, Tehran, Iran, Tel. +98 912 321 18 27; Fax: +98 21 66744339; emails: ahmahvi@yahoo.com (A.H. Mahvi), hamidz_14@yahoo.com (H. Zarei), naserise@tums.ac.ir (S. Nasseri), rnabizadeh@tums.ac.ir (R. Nabizadeh)*
[b]*Center for Water Quality Research, Institute for Environmental Research, Tehran University of Medical Sciences, Tehran, Iran*
[c]*Department of Chemical Engineering, Faculty of Chemical Engineering, University of Tehran, Tehran, Iran, email: shemiran@khayam.ut.ac.ir*
[d]*Environmental Science and Technology Research Center, Department of Environmental Health Engineering, School of Public Health, Shahid Sadoughi University of Medical Sciences, Yazd, Iran, email: arash.dalvand@gmail.com*
[e]*Center for Solid Waste Research, Institute for Environmental Research, Tehran University of Medical Sciences, Tehran, Iran*
[f]*National Institute of Health Research, Tehran University of Medical Sciences, Tehran, Iran*

Received 7 March 2015; Accepted 30 November 2016

ABSTRACT

In this study, response surface methodology (RSM) was employed for investigating the removal of As(V) from aqueous solution using multiwalled carbon nanotube (MWCNT)/alumina nanocomposite. The synthesized nanocomposite was characterized by scanning electron microscopy and X-ray diffraction. For conducting the experiments, four independent variables of initial As(V) concentration ranging from 0.1 to 0.9 mg L^{-1}, pH 3–11, contact time ranging from 15 to 1,450 min and adsorbent dose 0.5–1.5 g L^{-1} were selected and consecutively coded as X_1, X_2, X_3, and X_4 at three levels (−1, 0, and 1). A second-order polynomial regression model was then applied to predict responses. Regression analysis showed good fit of the experimental data to the second-order polynomial model with R^2 value of 0.9409 indicates the high correlation between observed and predicted values. At the optimum conditions that were initial As(V) concentration 0.5 mg L^{-1}, pH 7, contact time 80 min, and adsorbent dose 1 g L^{-1}, the As(V) removal efficiency was about 99.4%. This study proved that Box–Behnken design under RSM could efficiently be applied for modeling of As(V) removal by MWCNT/alumina nanocomposite.

Keywords: As(V) removal; Box–Behnken design; MWCNT/alumina nanocomposite

1. Introduction

Arsenic is the 20th most copious element in the earth's crust [1]. Arsenic pollution has been reported in the USA, Argentina, Hungary, China, Japan, Poland, Bangladesh, Mexico, Canada, New Zealand, Taiwan, and India [2–4]. Arsenic pollution is increasing throughout the world due to natural and increased anthropogenic activities [1]. Human activities that could increase arsenic concentrations in groundwaters and surface waters consist of waste incineration, electronics industries, oil and coal burning power plants, metal treatment, cement works, disinfectants, ammunition factories, household waste disposal, glassware production, pharmaceutical works, and galvanizing [5,6]. These effluents contain relatively high As(V) and trace As(III) concentration. In natural waters, it mainly presents in trivalent (H_3AsO_3, $H_2AsO_3^-$, and $HAsO_3^{2-}$) and pentavalent (H_3AsO_4, $HAsO_4^{2-}$, $H_2AsO_4^-$) oxidation states [7].

* Corresponding author.

Arsenic exposure may lead to neuropathy, hypertension, melanosis, and hyperkeratosis, and prolonged exposure to higher doses may lead to gangrene in the limbs skin cancer, lung, kidney, liver, and bladder cancers, and may be eventually fatal [8,9]. Because of toxicological influence of arsenic, the guideline value in drinking water is set as low as 10 μg L^{-1} by World Health Organization (WHO) in 1993 [10]. Various treatment techniques such as oxidation–reduction [11], ion flotation [12], co-precipitation [13], foam flotation precipitation [13], ion exchange [14,15], solvent extraction [14], bioremediation [12], electrolysis and cementation [16], electrocoagulation [17], and sorption [18] have been developed for the heavy metals remediation from drinking water. Adsorption process is a good alternative for pollutants removal [19] due to its ease of operation and handling [20], simplicity, sludge-free operation, high regeneration capacity, and removal efficiency. In recent years, various adsorbents such as zeolite [21], cellulose sponge [22], silica [23], phyllosilicates [23], activated alumina [24,25], sand [26], iron hydroxide [27,28], and activated carbon [29,30] have been utilized for remediation of arsenic from water. Alumina is the most promising adsorbent as it possesses excellent physical and textural properties compared with other transitional inorganic oxides [31].

Recently, application of nanoparticles for the removal of contaminants has come up as an attractive area of research because of exclusive characterization such as excellent adsorption efficiency especially due to higher surface area and greater active sites for interaction with metallic species [32]. Nanocomposites can be synthesized by a number of methods such as sol–gel, co-precipitation, and thermal decomposition [33,34]. The application of statistical experimental design techniques in adsorption process development can result in closer confirmation of the output response to nominal, reduced process variability, reduced development time, and overall costs [35]. Box–Behnken is a second-order multivariate design technique that the number of experiments (N) required for the progress of this design can be calculated according to the following equation:

$$N = 2k(k-1) + C_0 \quad (1)$$

where k is the number independent variables, and C_0 is the replicate number of the central point [36–38].

Multiwalled carbon nanotube (MWCNT) has been applied for removal of many pollutants [39]. According to literature review, the application of nanoalumina on MWCNT for removal of As(V) is not yet reported. Based on the abovementioned facts, the particular objectives of this study were: (1) utilization of three-level, four-factor Box–Behnken experimental design for modeling of As(V) removal from aqueous solution by MWCNT/alumina nanocomposite; (2) examination of the influence of four independent variables (As(V) concentration, pH of solution, contact time, and adsorbent dose) and their interactions on the As(V) removal efficiency; and (3) the confirmation of the validity of the proposed model.

2. Materials and methods

2.1. Materials

MWCNT, which was used as substrate for nanoalumina, was purchased from Research Institute of Petroleum Industry (Iran). According to supplier information, the purity, length, diameter, and specific surface area of the MWCNT were 95%, 10–30 nm, 10 μm, and 270 m^2/g, respectively.

All chemicals used in this work were obtained from Merck (Germany). All reagents used were of analytical reagent grade. Arsenate stock solution (1,000 mg L^{-1}) was prepared by dissolving 4.1653 g $Na_2HAsO_47H_2O$ into 1 L of deionized (DI) water. Working solutions were prepared fresh daily for each batch test. The batch experiments for the arsenate removal from aqueous solutions were carried out at room temperature, using DI water and suitable conical flasks (50 mL sample volume). The flasks were agitated on a reciprocal shaker (220 rpm) in different times. 1 M H_2SO_4 and NaOH were used for pH adjustment (pH meter: Jenway Model E520).

2.2. Synthesis of MWCNT/alumina nanocomposite

In order to synthesis the MWCNT/alumina nanocomposite, 1 g of MWCNT and 37.5 g of $Al(NO_3)_3$ were poured into a beaker containing 50 ml distilled water. Then, 2 ml of Triton X-100 was added in the mixture as surfactant and stirred for 2 h. While the mixture was stirring, sufficient amount of solid ammonium carbonate [$(NH_4)_2CO_3$] was added for complete precipitation. The mixture was stirred for 1 h at 100°C and left for precipitation for 3 d. The mixture was then filtered by a filter paper, and the residue was dried for 24 h at 60°C. The obtained solid material was ground in a mortar and then transferred to a flask. Approximately 25 ml of *n*-butanol was added into the flask, and sonication was applied for 45 min in order to dissolve the solid, and the solution was refluxed for 1 h to remove *n*-butanol. The obtained solid material was transferred into a porcelain crucible and then heated at about 800°C in argon atmosphere for about 1 h. The product was grey in color.

2.3. Characterization of MWCNT/alumina nanocomposite

Scanning electron microscopy (SEM) and X-ray diffraction (XRD) were used for the characterization of the synthesized nanocomposite. The photos of MWCNT/alumina nanocomposite were recorded using SEM (EM3200, Germany) at the accelerating voltage of 26 kV. The experimental conditions of XRD measurement were as follows: Cu Kα radiation; scanning range (2θ): 10°–109°, scanning speed 5°/min; and tube voltage/current, 40 kV/30 mA.

2.4. Box–Behnken design

Box–Behnken experimental design was found to be more suitable than other tested designs. Box–Behnken design allows to calculate the response function at intermediate levels and enables to estimate the system performance at any experimental point within the range studied through careful design and analysis of experiments [40]. The advantages of Box–Behnken designs comprise required factors to be run at only three levels, and designs are rotatable or nearly rotatable. Some of these designs also provide orthogonal blocking. In other words, in these designs, the block effects are orthogonal to the other factor effects [41,42]. In the present study, the three-level, four-factor Box–Behnken experimental design was applied to investigate and validate adsorption process variables affecting the removal of As(V) by MWCNT/alumina

nanocomposite. Initial As(V) concentration (0.1–0.9 mg L^{-1}), pH (3–11), contact time (15–145 min), and adsorbent dose (0.5–1.5 g L^{-1}) were chosen as the input variables and defined as X_1, X_2, X_3, and X_4, respectively. The factor levels were coded as −1 (low), 0 (central point or middle), and +1 (high). The variables and levels of the Box–Behnken design model are given in Table 1.

The results were analyzed using the R^2, analysis of variance (ANOVA), and response plots. A nonlinear regression was used to fit the second-order polynomial model (Eq. (2)). Response surface methodology (RSM) was applied to the experimental data using statistical Design-Expert software (version 7.0.0, trial).

The mathematical relationship of the response with the independent variables can be approximated by the quadratic polynomial equation:

$$Y = \beta_0 + \beta_1 X_1 + \beta_2 X_2 + \beta_3 X_3 + \beta_4 X_4 + \beta_{12} X_1 X_2 + \beta_{13} X_1 X_3 + \beta_{14} X_1 X_4 + \beta_{23} X_2 X_3 + \beta_{24} X_2 X_4 + \beta_{34} X_3 X_4 + \beta_{11} X_1^2 + \beta_{22} X_2^2 + \beta_{33} X_3^2 + \beta_{44} X_4^2 \quad (2)$$

where Y is the response; β_0 is the constant; β_1, β_2, β_3 and β_4 are the linear coefficients; β_{12}, β_{13}, β_{14}, β_{23}, β_{24}, and β_{34} are the interaction coefficients between the four factors; and β_{11}, β_{22}, β_{33}, and β_{44} are the quadratic coefficients. A total of 29 experiments have been carried out in this work to evaluate the effects of the four main independent variables on the As(V) removal efficiency. The Box–Behnken design matrix and the As(V) removal responses are given in Table 2.

Table 1
Levels of chosen variables in Box–Behnken design

Variable (unit)	Factors	Level		
		Low (−1)	Middle (0)	High (+1)
As(V) concentration (mg L^{-1})	X_1	0.1	0.5	0.9
pH	X_2	3	7	11
Time (min)	X_3	15	80	145
Adsorbent dose (g L^{-1})	X_4	0.5	1	1.5

Table 2
Box–Behnken design matrix for As(V) removal

Run no	Initial concentration (mg L^{-1})		pH		Contact time (min)		Adsorbent dose (g L^{-1})		Ar(V) removal efficiency (%)
	X_1 (coded)	X_1 (uncoded)	X_2 (coded)	X_2 (uncoded)	X_3 (coded)	X_3 (uncoded)	X_4 (coded)	X_4 (uncoded)	
1	–1	0.1	0	7	–1	15	0	1	99
2	–1	0.1	–1	3	0	80	0	1	99
3	+1	0.9	0	7	–1	15	0	1	91.2
4	+1	0.9	–1	3	0	80	0	1	98.33
5	0	0.5	0	7	–1	15	–1	0.5	84
6	+1	0.9	+1	11	0	80	0	1	47.11
7	0	0.5	+1	11	0	80	–1	0.5	53
8	0	0.5	–1	3	+1	145	0	1	97.2
9	–1	0.1	0	7	0	80	–1	0.5	99
10	–1	0.1	0	7	+1	145	0	1	99
11	0	0.5	+1	11	+1	145	0	1	52
12	0	0.5	0	7	0	80	0	1	99.4
13	–1	0.1	0	7	0	80	+1	1.5	99
14	+1	0.9	0	7	+1	145	0	1	99.11
15	0	0.5	0	7	0	80	0	1	99.4
16	0	0.5	0	7	+1	145	+1	1.5	98.6
17	0	0.5	+1	11	0	80	+1	1.5	43.6
18	0	0.5	+1	11	–1	15	0	1	43.2
19	+1	0.9	0	7	0	80	–1	0.5	83
20	0	0.5	–1	3	0	80	+1	1.5	95.8
21	–1	0.1	+1	11	0	80	0	1	10
22	0	0.5	–1	3	0	80	–1	0.5	92.6
23	0	0.5	0	7	–1	15	+1	1.5	98
24	0	0.5	–1	3	–1	15	0	1	97.2
25	0	0.5	0	7	0	80	0	1	99.4
26	+1	0.9	0	7	0	80	+1	1.5	98.55
27	0	0.5	0	7	0	80	0	1	99.4
28	0	0.5	0	7	0	80	0	1	99.4
29	0	0.5	0	7	+1	145	–1	0.5	97.6

2.5. Adsorption experiments

For each experiment, 50 ml of solution containing known concentration of As(V) and a known mass of the MWCNT/alumina nanocomposite were poured in a 100-ml conical flask. This mixture was agitated in room temperature on a reciprocating shaker at 220 rpm (Heidolph, Germany) for a specified time, and at a predetermined time interval, samples were taken and filtered (Whatman filter paper, 0.45 μm pore size). As(V) concentration in solution was determined using an Inductively Coupled Plasma Optical Emission Spectrometer (ICP–OES). Percentage of As(V) removal was calculated by the following equation:

$$\eta = \left[\left(C_0 - C\right)/C_0\right] \times 100 \quad (3)$$

where η is the As(V) removal efficiency (%), and C_0 and C are the concentration of As(V) before and after adsorption, respectively.

The phase distribution ratio (D) was calculated using the following equation:

$$D = \left(\frac{C_0 - C_f}{C_f}\right)\left(\frac{V}{W}\right) \quad (4)$$

where W is the weight of the nanocomposite in g, and V is the volume of the solution in mL.

3. Results and discussion

3.1. Characterization of MWCNT/alumina nanocomposite

The synthesized MWCNT/alumina nanocomposite was characterized by SEM and XRD. Fig. 1 shows SEM images of MWCNT and MWCNT/alumina nanocomposite. As shown in Figs. 1(a)–(c), the morphology of two surfaces is different. Surface analysis of two images indicated that the nanoalumina was successfully deposited on MWCNT surface, and the surface consists of small nanoparticles. In order to characterize the nature of synthesized material, XRD pattern of the material was also investigated. The XRD patterns revealed the presence of crystalline phases in the nanoadsorbent. According to the XRD pattern shown in Fig. 2, the existence of crystalline phases in nanoscale alumina on MWCNT can be ascertained by the appeared peaks at 2θ = 26°, 39°, 43°, and 78°, which are in good agreement with the reference pattern of alumina. Moreover, the peaks at 2θ = 26° and 52° correspond to MWCNT [43].

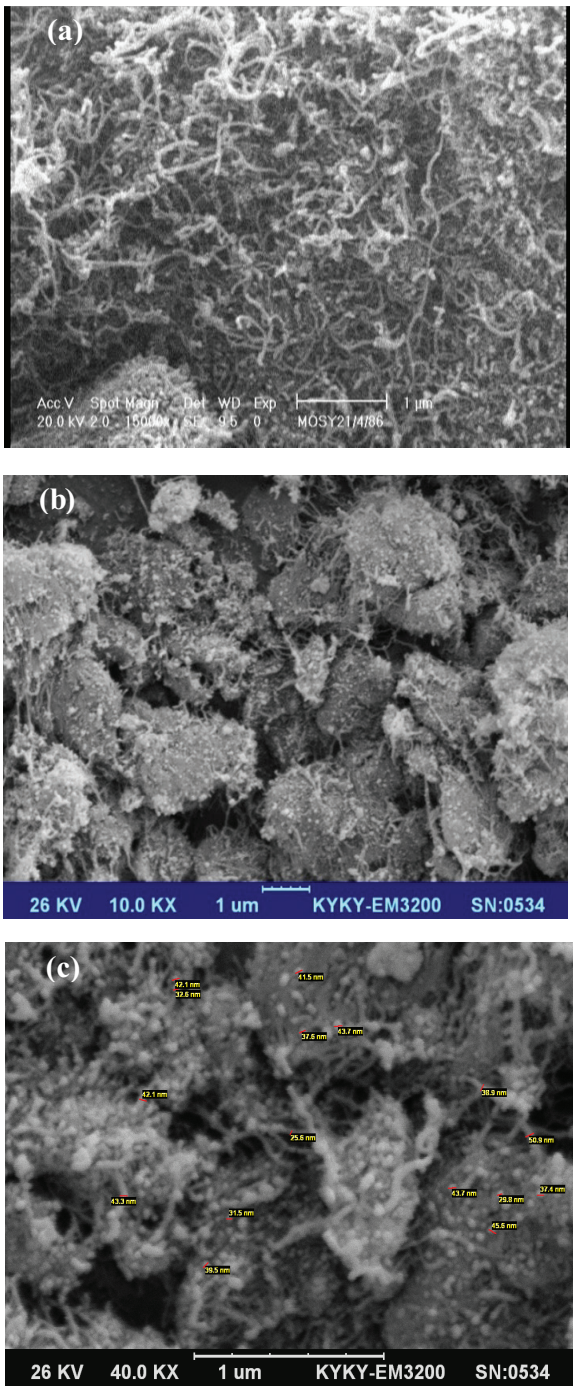

Fig. 1. (a) SEM micrograph of MWCNT, (b) SEM micrograph of MWCNT/alumina nanocomposite, and (c) SEM micrograph of MWCNT/alumina nanocomposite from a different angle.

3.2. Statistical model selection

In order to study the combined effect of different variables on As(V) removal, several variables that could potentially affect the efficiency of As(V) removal by the nanocomposite such as concentration of As(V), pH, contact time, and adsorbent dose were chosen [44].

In the present work, only two-way interactions were considered. Linear, interactive, quadratic, and cubic models were fitted to the experimental data to obtain the regression equations. To select the best model among various models, two different tests namely sequential model sum of squares and model summary statistics were carried out in the present study [45], and the results are given in Table 3. Sequential model sum of squares showed that the p value was lower than 0.01 for quadratic model only. As seen, the interaction of two factors (2FI) was not significant using the RSM [43]. Model summary statistics showed that the excluding cubic model, which was aliased, quadratic model, was found to have maximum "Adjusted R-Squared" and the "Predicted R-Squared" values. Therefore, quadratic model was chosen for further analysis.

3.3. Fitting of statistical analysis and second-order polynomial equation

The RSM offers an empirical relationship between the response function and the independent variables. An empirical relationship between the experimental results obtained on the basis of Box–Behnken experimental design model and the input variables was expressed by a second-order polynomial model in Eq. (5):

$$Y = +99.40 + 1.02X_1 - 27.6X_2 + 2.68X_3 + 2.13X_4 + 9.45X_1X_2 + 1.98X_1X_3 + 3.89X_1X_4 + 2.2X_2X_3 - 3.15X_2X_4 - 2.94X_3X_4 - 4.26X_1^2 - 28.42X_2^2 + 0.12X_3^2 - 1.55X_4^2 \quad (5)$$

where Y is the predicted As(V) removal efficiency; X_1, X_2, X_3, and X_3 are the coded terms for four independent variables of initial As(V) concentration, pH, contact time, and adsorbent dose, respectively.

Sen and Swaminathan [46] have reported that the ANOVA is essential to test the significance of the model. ANOVA is a statistical technique that subdivides the total variation in a set of data into component parts associated with specific sources of variation for the purpose of testing hypotheses on the variables of the model [47]. The ANOVA was conducted to test the fitness of the second-order polynomial equation for the experimental data as given in Table 4. As seen in Table 4, a very low probability value (p value < 0.0001) suggests that the quadratic model is highly significant [48]. The large value of F signifies that the terms in the model have a substantial impact on the response. The probability (<0.0001) is less than 0.05. This illustrate that the model terms are statistically significant at 95% of probability level [49]. Any factor or interaction of factors with p value < 0.05 is significant.

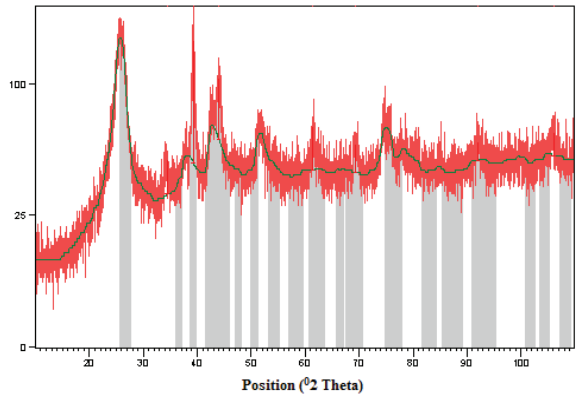

Fig. 2. XRD pattern of MWCNT/alumina nanocomposite.

The fitness of the model was checked by coefficient of determination (R^2). In this case, the value of R^2 = 0.9409 (Fig. 3) illustrates that only 5.91% of the total variations were not elucidation by the regression model. The value of adjusted R^2 (adjusted R^2 = 0.8772) was also high; this illustrates high correlation between the observed and the predicted values, as similarly reported by other researchers [48,50,51]. Liu et al. [48] have reported that the adjusted R^2 corrects the R^2 value for the sample size and the number of terms in the model. In our case, the adjusted R^2 was found to be close to the R^2 value. The coefficient of variation (CV = 10.08%) implies that the model is highly significant and experiments are highly reliable and accurate [46,50].

Adequate precision measures the signal-to-noise ratio. A ratio greater than 4 is desirable. For the present study, signal-to-noise ratio was found to be 11.84, which indicates the adequate signal. The As(V) removals measured for the different batch experiments showed an extensive variation ranging from a minimum of 10% to a maximum of 99.4%. Results obviously showed that the As(V) removal efficiency was strongly affected by the selected independent variables.

Data were also analyzed to check the normality of the residuals. A normal probability plot of the residuals is shown in Fig. 4. The data pointed on this plot lie reasonably close to a straight line that confirms the normal distribution of errors and adequacy of the model [52].

3.4. Three-dimensional response surface and contour plots

Three-dimensional (3D) response surface and contour plots can easily illustrate the effects of the experimental variables on the responses [53]. Adinarayana and Ellaiah [50]

Table 3
Adequacy of the model tested

Source	Sum of squares	Degrees of freedom (df)	Mean square	F value	p value prob > F	Remark
Mean	2.012E+005	1	2.012E+005			
Linear	9,194.97	4	2,298.74	7.71	0.0004	
2FI	700.75	6	116.79	0.32	0.9162	
Quadratic	5,208.90	4	1,302.23	17.84	<0.0001	Suggested
Cubic	948.10	8	118.51	547.85	<0.0001	Aliased
Residual	1.08	5	0.22			
Total	2.173E+005	28	7,758.94			
Source	Standard deviation	Predicted R^2	Adjusted R^2	R^2	PRESS	Remark
Linear	17.27	0.5728	0.4985	0.3541	10,369.20	
2FI	19.03	0.6164	0.3908	–0.1632	18,673.42	
Quadratic	8.54	0.9409	0.8772	0.6095	6,268.82	Suggested
Cubic	0.47	0.9999	0.9996	–0.11	18,026	Aliased

Table 4
ANOVA results for As(V) adsorption by MWCNT/alumina nanocomposite

Source	Sum of squares	Degrees of freedom (df)	Mean square	*F* value	*p* value prob > *F*	Remark
Model	15,104.63	14	1,078.90	14.78	<0.0001	Significant
X_1–concentration	12.61	1	12.61	0.17	0.6845	
X_2–pH	9,142.22	1	9,142.22	125.21	<0.0001	Significant
X_3–time	71.82	1	71.82	0.98	0.3394	
X_4–dose	45.51	1	45.51	0.62	0.4440	
$X_1 \times X_2$	356.83	1	356.83	4.89	0.0456	Significant
$X_1 \times X_3$	15.64	1	15.64	0.21	0.6511	
$X_1 \times X_4$	60.45	1	60.45	0.83	0.3794	
$X_2 \times X_3$	19.36	1	19.36	0.27	0.6152	
$X_2 \times X_4$	39.69	1	39.69	0.54	0.4740	
$X_3 \times X_4$	21.57	1	21.57	0.30	0.5959	
X_1^2	114.64	1	114.64	1.57	0.2323	
X_2^2	5,100.49	1	5,100.49	69.86	<0.0001	Significant
X_3^2	0.087	1	0.087	1.195E-003	0.9729	
X_4^2	14.03	1	14.03	0.19	0.6684	
Residual	949.18	13	73.01			
Lack of fit	949.18	9	105.46			
Pure error	0.000	4	0.000			
Cor. Total	16,053.81	27				

Note: R^2 = 0.9409, adjusted R^2 = 0.8772, adequate precision = 11.84, and CV = 10.08%.

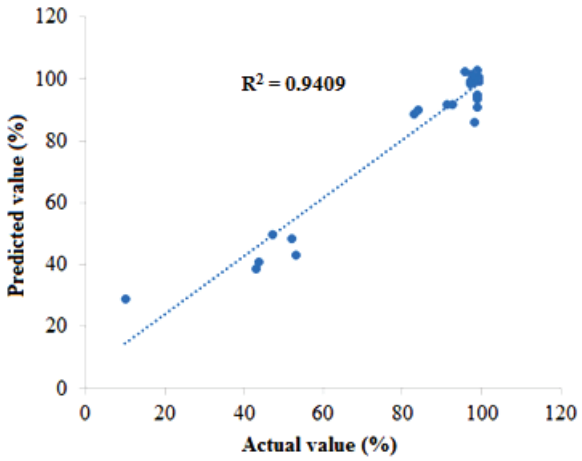

Fig. 3. Regression plot of the actual results vs. predicted data for As(V) adsorption by MWCNT/alumina nanocomposite.

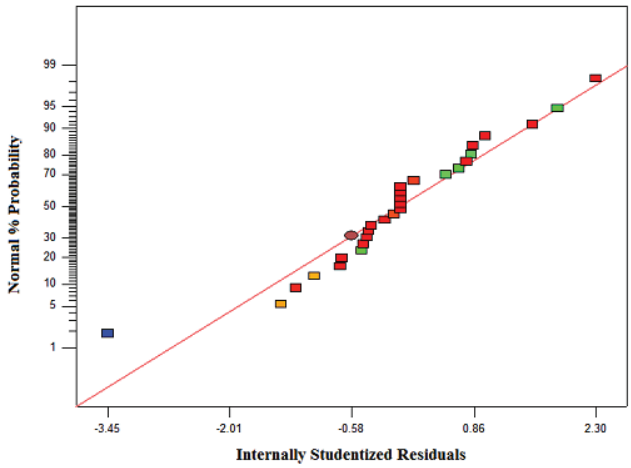

Fig. 4. Normal probability plot for As(V) adsorption.

have reported 3D response surface plots with maintaining all other factors at constant levels are useful in perception of main and the interplay effect of two factors. By applying contour plots, the relation between the dependent and independent variables was also described. Since the regression model has four independent variables (two variables were held constant at the center level for each plot), a total of four 3D plots and contour plots were presented for responses. Figs. 5 and 6 show the 3D response surfaces and the corresponding contour plots as the functions of two variables, respectively. The nonlinear nature of all 3D response surfaces and the respective contour plots proved that there were noticeable interactions between each of the independent variables and the As(V) removal efficiency.

3.5. Effect of independent variables on As(V) removal efficiency

To study the effect of adsorbent dose and contact time on As(V) removal, experiments were carried out by varying adsorbent dose from 0.5 to 1.5 g L^{-1} under different contact time ranging from 15 to 145 min, and the results are plotted in Figs. 5 and 6. These figures clearly show that the removal of As(V) increases with an increase in adsorbent dose and contact time (Figs. 5(a) and (b)). This result can be attributed

to greater surface area and the availability of more adsorption sites at higher adsorbent dose [54]. Similar trend has been reported for cadmium removal [55].

The highest As(V) removal was attained at the adsorbent dose of 1 g L^{-1} and contact time of 80 min. Enough adsorbent dose and contact time provide opportunity to As(V) ions diffuse deeper into the adsorbent structure at highest energy sites [56,57].

The effect of initial As(V) concentration and pH on the As(V) removal at various initial As(V) concentrations from 0.1 to 0.9 mg L^{-1} and pH from 3 to 11 is plotted in Figs. 5 and 6. As shown in Figs. 5(a) and (c), by increasing As(V)

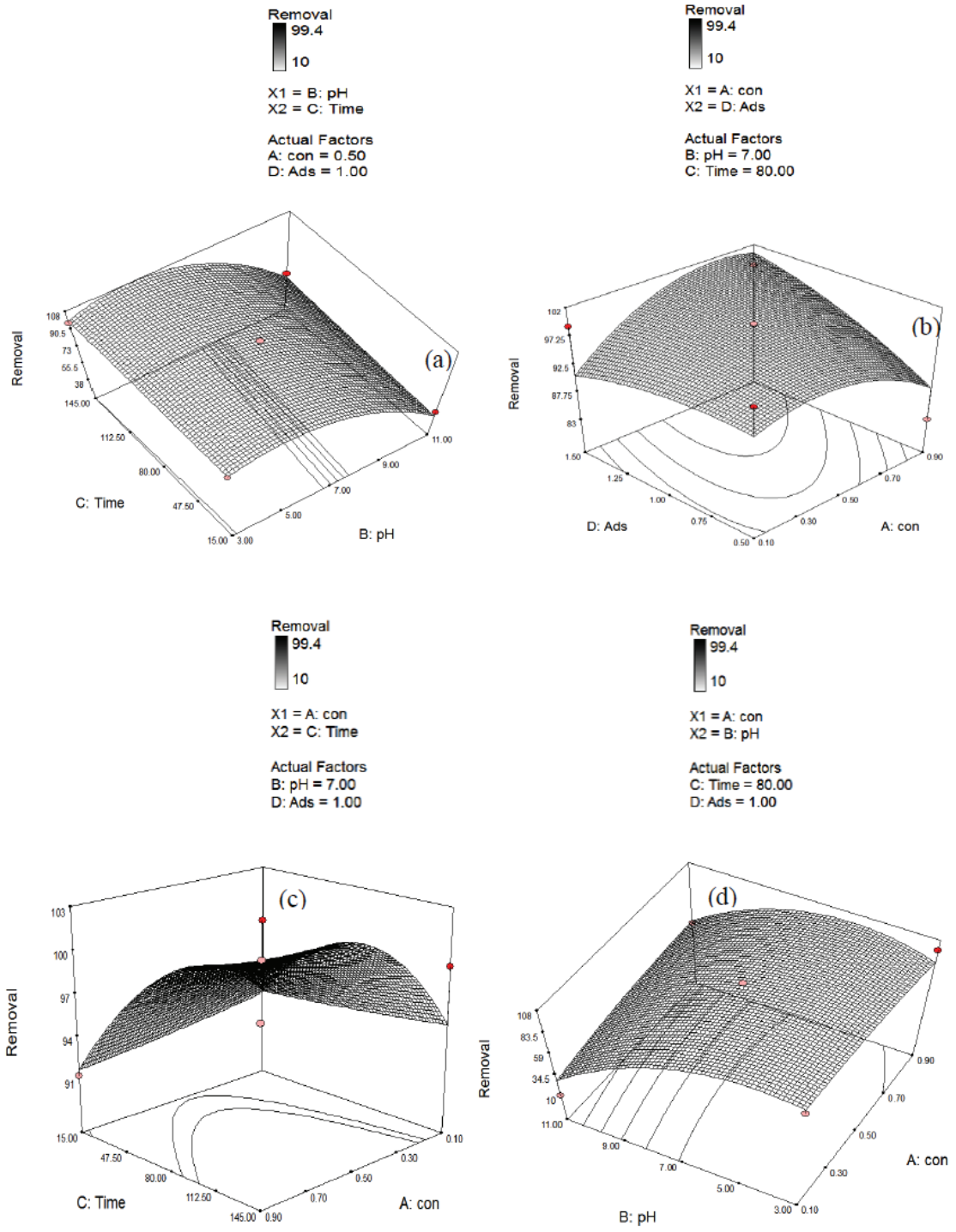

Fig. 5. 3D response surface diagrams of As(V) removal as the function of independent variables: (a) pH–contact time, (b) As(V) concentration–adsorbent dose, (c) As(V) concentration–contact time, and (d) As(V) concentration–pH.

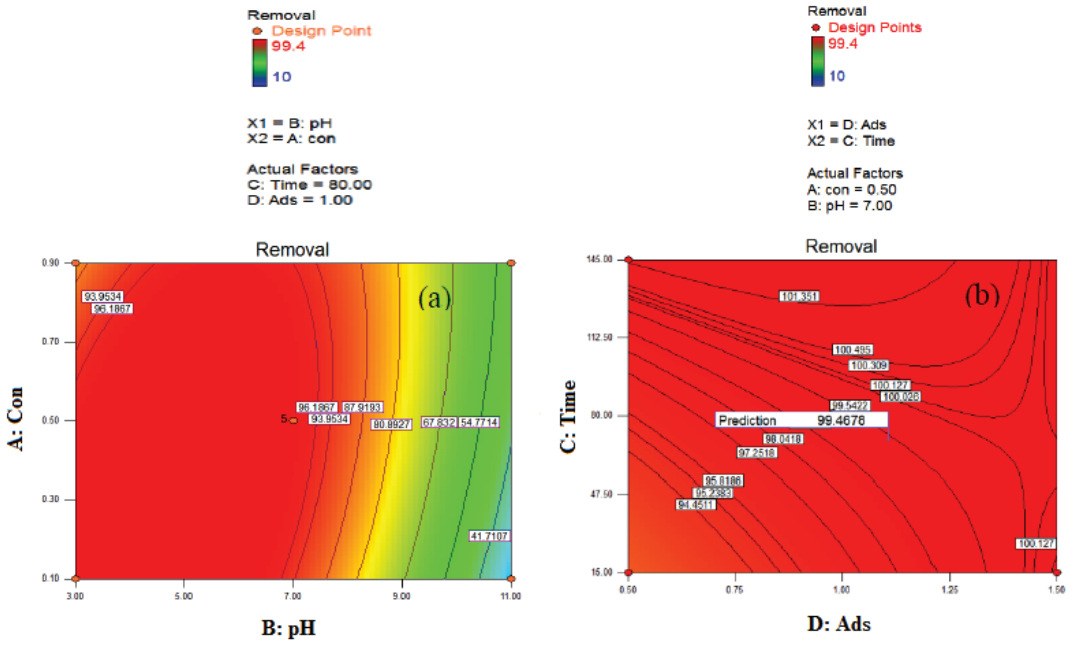

Fig. 6. Contour plots of As(V) removal as the function of independent variables (other variables were held at their respective center levels): (a) concentration of As(V)–pH and (b) adsorbent dose–contact time.

concentration, its removal decreases. This result is due to the lack of ample availabe adsorption sites for adsorption of all As(V) ions [52]. At pH below 8, the surface of alumina has positive charge [58]. Threfore, as the pH of solution raises from 3 to 11, the number of the positively charged sites on the nanocomposite surface decreases, and As(V) removal decreases (Figs. 5(a) and 6(a)). At pH above 7, the number of the negatively charged sites on the surface of adsorbent increases. Lower adsorption of As(V) at higher pH is due to the presence of excess OH^- ions in the solution that compete with the As(V) anions for the adsorption sites.

Morover, at pH between 3 and 6, $H_2AsO_4^-$ is dominant species of As(V) in the solution, while $HAsO_4^{-2}$ is dominant at higher pH values [58]. At pH 7, the adsorption of As(V) is higher due to electrostatic interaction between $HAsO_4^{-2}$, which has high negative charge, and the nanocomposite, which has positive charge. Similar findings have been observed by Han et al. for As(V) removal using mesoporous alumina [59].

Therefore, it can be said that As(V) removal decreases with increasing pH and initial As(V) concentration, while increases with contact time and adsorbent dose.According to the ANOVA results, the pH has more profound effect on As(V) removal as compared with contact time and adsorbent dose.

3.6. Selection of optimal levels for As(V) removal

The aim of optimization was to achieve the maximum As(V) removal using the lowest adsorbent amount. Table 5 summarizes the optimal level of various variables obtained after examining the response curves and contour plots. On the basis of the calculation steps defined for the optimization algorithm, the optimal values of the tested variables in uncoded units were found to be the initial As(V) concentration 0.5 mg L^{-1}, pH 7, contact time 80 min, and the adsorbent dose 1 g L^{-1}. At the optimal condition, the experimental As(V) removal was 99.4%, which was near to the predicted value of 99.39.

Table 5
Optimum values of independent variable for maximum As(V) removal efficiency

Variable	Optimum value	
	Predicted values	Experimental values
As(V) removal (%)	99.3999	99.4
As(V) concentration (mg L^{-1})	0.5	0.5
pH	7	7
Time (min)	80	80
Adsorbent dose (g L^{-1})	1	1

4. Conclusion

In this study, the Box–Behnken model under the RSM was used to examine the role of four independent variables on As(V) removal by the MWCNT/alumina nanocomposite. The proposed mathematical methodology also provided a critical analysis of the simultaneous interactive effects of independent variables, such as initial As(V) concentration, pH, contact time, and adsorbent dose for better understanding of the As(V) removal process. The predicted values obtained using the quadratic model were in very good agreement with the experimental values (R^2 = 0.9409, adjusted R^2 = 0.8772, adequate precision = 11.84, and CV = 10.08%). The optimum values of variables to attain the highest As(V) removal were found to be initial As(V) concentration of 0.5 mg L^{-1}, pH 7,

contact time 80 min, and adsorbent dose 1 g L^{-1}. The maximum adsorption of As(V) was 99.4%. Therefore, this study showed that the Box–Behnken model is suitable to optimize the experiments for As(V) removal, suggesting that the MWCNT/alumina nanocomposite can be applied as an ideal adsorbents for the practical water treatment application.

Acknowledgment

This study was financially supported by Center for Water Quality Research, Institute for Environmental Research, and Tehran University of Medical Sciences (Grant No,: 92-03-46-24557). The authors would like to thank staff of laboratory, Department of Environmental Health Engineering, School of public Health, and Faculty of Chemistry.

References

[1] W.R. Cullen, K.J. Reimer, Arsenic speciation in the environment, Chem. Rev., 89 (1989) 713–764.
[2] S.L. Chen, S.R. Dzeng, M.H. Yang, K.H. Chiu, G.M. Shieh, C.M. Wai, Arsenic species in groundwaters of the blackfoot disease area, Taiwan, Environ. Sci. Technol., 28 (1994) 877–881.
[3] M. Karim, Arsenic in groundwater and health problems in Bangladesh, Water Res., 34 (2000) 304–310.
[4] D. Chakraborti, M.M. Rahman, K. Paul, U.K. Chowdhury, M.K. Sengupta, D. Lodh, C.R. Chanda, K.C. Saha, S.C. Mukherjee, Arsenic calamity in the Indian subcontinent: what lessons have been learned? Talanta, 58 (2002) 3–22.
[5] J. Matschullat, Arsenic in the geosphere – a review, Sci. Total Environ., 249 (2000) 297–312.
[6] M. Berg, H.C. Tran, T.C. Nguyen, H.V. Pham, R. Schertenleib, W. Giger, Arsenic contamination of groundwater and drinking water in Vietnam: a human health threat, Environ. Sci. Technol., 35 (2001) 2621–2626.
[7] A. Ohki, K. Nakayachigo, K. Naka, S. Maeda, Adsorption of inorganic and organic arsenic compounds by aluminium-loaded coral limestone, Appl. Organomet. Chem., 10 (1996) 747–752.
[8] J.M. Neff, Ecotoxicology of arsenic in the marine environment, Environ. Toxicol. Chem., 16 (1997) 917–927.
[9] S. Ouvrard, M.O. Simonnot, M. Sardin, Reactive behavior of natural manganese oxides toward the adsorption of phosphate and arsenate, Ind. Eng. Chem. Res., 41 (2002) 2785–2791.
[10] WHO, Guidelines for Drinking-water Quality, third ed., World Health Organization, Geneva, 2006.
[11] K. Van Hege, M. Verhaege, W. Verstraete, Electro-oxidative abatement of low-salinity reverse osmosis membrane concentrates, Water Res., 38 (2004) 1550–1558.
[12] I.A. Katsoyiannis, A.I. Zouboulis, Application of biological processes for the removal of arsenic from groundwaters, Water Res., 38 (2004) 17–26.
[13] P. Mondal, C. Majumder, B. Mohanty, Laboratory based approaches for arsenic remediation from contaminated water: recent developments, J. Hazard. Mater., 137 (2006) 464–479.
[14] J. Kim, M.M. Benjamin, Modeling a novel ion exchange process for arsenic and nitrate removal, Water Res., 38 (2004) 2053–2062.
[15] L. Rafati, A.H. Mahvi, A. Asgari, S.S. Hosseini, Removal of chromium (VI) from aqueous solutions using Lewatit FO 36 nano ion-exchange resin, Int. J. Environ. Sci. Technol., 7 (2010) 147–156.
[16] N. Balasubramanian, K. Madhavan, Arsenic removal from industrial effluent through electrocoagulation, Chem. Eng. Technol., 24 (2001) 519–521.
[17] E. Bazrafshan, A.H. Mahvi, S. Naseri, A.R. Mesdaghinia, Performance evaluation of electrocoagulation process for removal of chromium (VI) from synthetic chromium solutions using iron and aluminum electrodes, Turk. J. Eng. Environ. Sci., 32 (2008) 59–66.
[18] S. Atkinson, Filtration technology verified to remove arsenic from drinking water, Membr. Technol., 2006 (2006) 8–9.
[19] V. Lenoble, V. Deluchat, B. Serpaud, J.C. Bollinger, Arsenite oxidation and arsenate determination by the molybdene blue method, Talanta, 61 (2003) 267–276.
[20] A.H. Mahvi, Application of agricultural fibers in pollution removal from aqueous solution, Int. J. Environ. Sci. Technol., 5 (2008) 275–285.
[21] M.S. Onyango, Y. Kojima, H. Matsuda, A. Ochieng, Adsorption kinetics of arsenic removal from groundwater by iron-modified zeolite, J. Chem. Eng. Jpn., 36 (2003) 1516–1522.
[22] J.A. Munoz, A. Gonzalo, M. Valiente, Arsenic adsorption by Fe(III)-loaded open-celled cellulose sponge. Thermodynamic and selectivity aspects, Environ. Sci. Technol., 36 (2002) 3405–3411.
[23] Y. Xu, L. Axe, Synthesis and characterization of iron oxide-coated silica and its effect on metal adsorption, J. Colloid Interface Sci., 282 (2005) 11–19.
[24] T.S. Singh, K. Pant, Equilibrium, kinetics and thermodynamic studies for adsorption of As(III) on activated alumina, Sep. Purif. Technol., 36 (2004) 139–147.
[25] S. Kuriakose, T.S. Singh, K.K. Pant, Adsorption of As(III) from aqueous solution onto iron oxide impregnated activated alumina, Water Qual. Res. J. Can., 39 (2004) 258–266.
[26] S.L. Lo, H.T. Jeng, C.H. Lai, Characteristics and adsorption properties of iron-coated sand, Water Sci. Technol., 35 (1997) 63–70.
[27] W. Driehaus, M. Jekel, U. Hildebrandt, Granular ferric hydroxide-a new adsorbent for the removal of arsenic from natural water, J. Water Supply Res. Technol. AQUA, 47 (1998) 30–35.
[28] C. Appelo, M. Van der Weiden, C. Tournassat, L. Charlet, Surface complexation of ferrous iron and carbonate on ferrihydrite and the mobilization of arsenic, Environ. Sci. Technol., 36 (2002) 3096–3103.
[29] R.L. Vaughan Jr., B.E. Reed, Modeling As(V) removal by a iron oxide impregnated activated carbon using the surface complexation approach, Water Res., 39 (2005) 1005–1014.
[30] Z. Gu, J. Fang, B. Deng, Preparation and evaluation of GAC-based iron-containing adsorbents for arsenic removal, Environ. Sci. Technol., 39 (2005) 3833–3843.
[31] H. Takanashi, A. Tanaka, T. Nakajima, A. Ohki, Arsenic removal from groundwater by a newly developed adsorbent, Water Sci. Technol., 50 (2004) 23–32.
[32] K. Hristovski, A. Baumgardner, P. Westerhoff, Selecting metal oxide nanomaterials for arsenic removal in fixed bed columns: from nanopowders to aggregated nanoparticle media, J. Hazard. Mater., 147 (2007) 265–274.
[33] H. Gleiter, Nanostructured materials: basic concepts and microstructure, Acta Mater., 48 (2000) 1–29.
[34] H.C. Lee, H.J. Kim, C.H. Rhee, K.H. Lee, J.S. Lee, S.H. Chung, Synthesis of nanostructured γ-alumina with a cationic surfactant and controlled amounts of water, Microporous Mesoporous Mater., 79 (2005) 61–68.
[35] G. Annadurai, R.-S. Juang, D.J. Lee, Factorial design analysis for adsorption of dye on activated carbon beads incorporated with calcium alginate, Adv. Environ. Res., 6 (2002) 191–198.
[36] S. Buco, M. Moragues, M. Sergent, P. Doumenq, G. Mille, An experimental design approach for optimizing polycyclic aromatic hydrocarbon analysis in contaminated soil by pyrolyser-gas chromatography-mass spectrometry, Environ. Res., 104 (2007) 209–215.
[37] M. Sivakumar, G. Annadurai, D. Mohan, Studies on Box-Behnken design experiments: cellulose acetate-polyurethane ultrafiltration membranes for BSA separation, Bioprocess. Eng., 21 (1999) 65–68.
[38] M. Soylak, I. Narin, M.d.A. Bezerra, S.L.C. Ferreira, Factorial design in the optimization of preconcentration procedure for lead determination by FAAS, Talanta, 65 (2005) 895–899.
[39] M. Shirmardi, A. Mesdaghinia, A.H. Mahvi, S. Nasseri, R. Nabizadeh, Kinetics and equilibrium studies on adsorption of acid red 18 (azo-dye) using multiwall carbon nanotubes (MWCNTs) from aqueous solution, E-J. Chem., 9 (2012) 2371–2383.

[40] E. Hamed, A. Sakr, Application of multiple response optimization technique to extended release formulations design, J. Control. Release, 73 (2001) 329–338.
[41] J.T. Batalon, P.S. Madamba, PH—postharvest technology: optimization of coir dust compaction using the response surface methodology approach, J. Agric. Eng. Res., 78 (2001) 167–175.
[42] A.B. Solanki, J.R. Parikh, R.H. Parikh, Formulation and optimization of piroxicam proniosomes by 3-factor, 3-level Box-Behnken design, AAPS PharmSciTech., 8 (2007) 43–49.
[43] V.K. Gupta, S. Agarwal, T.A. Saleh, Synthesis and characterization of alumina-coated carbon nanotubes and their application for lead removal, J. Hazard. Mater., 185 (2011) 17–23.
[44] I.D. Mall, V.C. Srivastava, N.K. Agarwal, Adsorptive removal of Auramine-O: kinetic and equilibrium study, J. Hazard. Mater., 143 (2007) 386–395.
[45] M. Muthukumar, D. Mohan, M. Rajendran, Optimization of mix proportions of mineral aggregates using Box Behnken design of experiments, Cem. Concr. Compos., 25 (2003) 751–758.
[46] R. Sen, T. Swaminathan, Response surface modeling and optimization to elucidate and analyze the effects of inoculum age and size on surfactin production, Biochem. Eng. J., 21 (2004) 141–148.
[47] L. Huiping, Z. Guoqun, N. Shanting, L. Yiguo, Technologic parameter optimization of gas quenching process using response surface method, Comput. Mater. Sci., 38 (2007) 561–570.
[48] H.L. Liu, Y.W. Lan, Y.C. Cheng, Optimal production of sulphuric acid by *Thiobacillus thiooxidans* using response surface methodology, Process Biochem., 39 (2004) 1953–1961.
[49] J. Segurola, N.S. Allen, M. Edge, A. Mc Mahon, Design of eutectic photoinitiator blends for UV/visible curable acrylated printing inks and coatings, Prog. Org. Coat., 37 (1999) 23–37.
[50] K. Adinarayana, P. Ellaiah, Response surface optimization of the critical medium components for the production of alkaline protease by a newly isolated Bacillus sp, J. Pharm. Pharm. Sci., 5 (2002) 272–278.
[51] M.Y. Can, Y. Kaya, O.F. Algur, Response surface optimization of the removal of nickel from aqueous solution by cone biomass of *Pinus sylvestris*, Bioresour. Technol., 97 (2006) 1761–1765.
[52] A. Dalvand, R. Nabizadeh, M.R. Ganjali, M. Khoobi, S. Nazmara, A.H. Mahvi, Modeling of reactive blue 19 azo dye removal from colored textile wastewater using l-arginine-functionalized Fe_3O_4 nanoparticles: optimization, reusability, kinetic and equilibrium studies, J. Magn. Magn. Mater., 404 (2016) 179–189.
[53] D. Wu, J. Zhou, Y. Li, Effect of the sulfidation process on the mechanical properties of a CoMoP/Al_2O_3 hydrotreating catalyst, Chem. Eng. Sci., 64 (2009) 198–206.
[54] A. Maleki, A.H. Mahvi, M.A. Zazouli, H. Izanloo, A.H. Barati, Aqueous cadmium removal by adsorption on barley hull and barley hull ash, Asian J. Chem., 23 (2011) 1373–1376.
[55] A.H. Mahvi, F. Gholami, S. Nazmara, Cadmium biosorption from wastewater by Ulmus leaves and their ash, Eur. J. Sci. Res., 23 (2008) 197–203.
[56] V.S. Mane, I.D. Mall, V.C. Srivastava, Use of bagasse fly ash as an adsorbent for the removal of brilliant green dye from aqueous solution, Dyes Pigm., 73 (2007) 269–278.
[57] P. Tripathi, V.C. Srivastava, A. Kumar, Optimization of an azo dye batch adsorption parameters using Box-Behnken design, Desalination, 249 (2009) 1273–1279.
[58] Y. Kim, C. Kim, I. Choi, S. Rengaraj, J. Yi, Arsenic removal using mesoporous alumina prepared via a templating method, Environ. Sci. Technol., 38 (2004) 924–931.
[59] C. Han, H. Li, H. Pu, H. Yu, L. Deng, S. Huang, Y. Luo, Synthesis and characterization of mesoporous alumina and their performances for removing arsenic (V), Chem. Eng. J., 217 (2013) 1–9.